This is the author's version of an article that has been published in this journal. Changes were made to this version by the publisher prior to publication.
The final version of record is available at http://dx.doi.org/10.1109/TSG.2018.2825103

Coordinated Operation of Electricity and Natural Gas Systems: A Convex Relaxation Approach

Saeed D. Manshadi, *Student Member IEEE*, Mohammad E. Khodayar, *Senior Member, IEEE*

***Abstract*—The variability in the generation dispatch of the natural gas generation units will lead to fluctuation in natural gas demand profile that could further jeopardize the security of the natural gas network. The coordinated operation of electricity and natural gas infrastructure systems would help to improve the security and reliability measures in both infrastructure systems and mitigate the risk of demand curtailment. The electricity and natural gas network operation problems are non-convex mixed-integer nonlinear programming problems that are hard to solve in polynomial time. The non-convex feasible regions are formed by the Weymouth constraint and the introduced binary commitment decision variables in the natural gas and electricity network operation problems respectively. This paper utilized a sparse semidefinite programming (SDP) relaxation to procure the optimal solution for the coordinated operation of electricity and natural gas networks. The presented algorithm leverages the sparseness of the natural gas network to construct several small matrices of lifting variables that are used to form a tight and traceable SDP relaxation. A set of valid constraints that tighten the relaxation ensures the exactness of the solution procured from the relaxed problem. The effectiveness of the presented approach is shown in case studies.**

***Index Terms*— Convex relaxation, coordinated operation, natural gas network, unit commitment.**

NOMENCLATURE

<u>Variables and Indices:</u>

b	Index for electricity network bus
$f_{j,o}^{p,t}$	Natural gas flow in pipeline p among junctions j and o
$I_{i,t}$	Commitment decision of unit i at hour t; 1 if the unit is ON and 0 otherwise
i	Index for generation unit
j,o	Index for natural gas network junction
k	Index for non-electric natural gas consumption
l	Index for transmission line
p	Index for natural gas pipelines
$P_{i,t}$	Power generation dispatch of unit i at hour t
s	Index for the natural gas resources
t	Index for hour
$v_{s,t}$	Natural gas withdrawal from resource s at hour t
$X_{i,t}^{on}$	On time of unit i at hour t
$X_{i,t}^{off}$	Off time of unit i at hour t
$\alpha_i, \beta_i, \gamma_i$	Fuel cost coefficients of generation unit i
$\pi_{j,t}$	Natural gas pressure at junction j at hour t

<u>Constants:</u>

A_j^s	Natural gas junction-resource incidence matrix
B_b	Set of units that are connected to bus b
$C_{j,o}^p$	Pipeline constant
$f_{j,o}^{p,\max}$	Maximum natural gas flow capacity of pipeline p
$\bar{F}_l$	Maximum capacity of transmission line l
GG_j	Set of natural gas-fired units connected to junction j
GS_j	Set of natural gas resources connected to junction j
$H_i(.)$	Natural gas consumption function for natural gas generation unit i
HH_j	Set of non-electric natural gas demands connected to junction j
NB	Total number of buses
NG	Total number of natural gas generation units
NL	Total number of transmission lines
NP	Total number of natural gas pipelines
NJ	Total number of natural gas junctions
$P_{k,t}^h$	Non-electric natural gas demand k at hour t
$P_{b,t}^D$	Electricity demand in bus b at hour t
$P_{f,j}$	Set of pipelines starting from junction j
$P_{t,j}$	Set of pipelines ending at junction j
$\bar{P}_i, \underline{P}_i$	Maximum/minimum generation capacity of unit i
RU_i	Maximum ramping up of unit i
RD_i	Maximum ramping down of unit i
SF_l^b	Shift factor of line l with respective to bus b
T_i^{on}, T_i^{off}	Minimum up/down time of unit i

Saeed D. Manshadi and Mohammad Khodayar are with department of electrical engineering, Southern Methodist University, Dallas, TX. (e-mails: manshadi@smu.edu, mkhodayar@smu.edu).

$\Gamma_{j,o}^{p}$ Maximum compression ratio for natural gas pipeline p
ξ_s Cost of natural gas supply at source s
$\underline{\pi}, \overline{\pi}$ Minimum/Maximum natural gas pressure
$\overline{v}_s, \underline{v}_s$ Max/min natural gas withdrawal of resource s

I. Introduction

Several research efforts addressed the interdependence among natural gas and electricity networks [1]-[2]. In the electricity network, the natural gas generation units are fast response units that compensate for the generation scarcity that is triggered by sudden changes in the renewable generation dispatch or the electricity demand. The essence of capturing natural gas constraints in bulk-power and distribution network operations is addressed in [3] and [4]. Some research works ignored the network model for the electricity or natural gas system and addressed the economic and environmental objectives/constraints by simply balancing the demand and supply using single-node approach [5]-[6]. Other research works highlighted the challenges associated with the non-convexity of the network models [4] by presenting a linear representation [7], a multi-dimensional piecewise linear approximation [8], adaptive partitioning [9], or successive linear formulation [10] to convexify the network constraints and to determine an equilibrium point [11] for the overall energy flow. These approaches require a large number of piecewise estimates and a considerable number of iterations for accurate piecewise linear approximation, while there is no guarantee for the exact solution. In [12], a security-constrained unit commitment problem is solved using Benders decomposition approach in which the constraints of the natural gas network are incorporated in the sub-problem. The methodology proposed in [12] to solve the nonlinear and nonconvex natural gas operation sub-problem is an iterative procedure with a predefined tolerance for error, and Benders decomposition is used to ensure the feasibility of the natural gas network constraints. Other research efforts leveraged heuristic approaches such as genetic algorithm [13] to solve for the energy flows in the interdependent electricity and natural gas networks. Similar convexification, linearization [14], and heuristic approaches [15] were used for the expansion planning practices in the electricity and natural gas networks. Several scenarios for coordination among the electricity and natural gas networks are investigated in [16] to improve the economic and security measures. An important notion which was ignored in earlier research is that the electricity and natural gas systems are usually operated by different entities with heterogeneous objectives [17]. Therefore, the short-term and long-term operational planning for these interdependent infrastructure systems should capture the limitations on the shared information among their respective system operators [18]. A consensus operation framework facilitates the coordinated operation of electricity and natural gas networks. The benefits of the consensus-based distributed approach over the Lagrange relaxation are presented in [19]. In order to guarantee the convergence, the short-term operation problem for each infrastructure system is required to be formulated as a convex optimization problem [18].

In the natural gas network, the flow in the pipelines is formulated by a nonconvex Weymouth constraint and in order to convexify this constraint, the direction of natural gas flow in the pipeline is assumed as known and unchanged [18]. This assumption may not be valid as the direction of the natural gas flow in the pipeline may change suddenly to supply the natural gas generation units and compensate for the variability of renewable generation in electricity networks [20],[21]. The variability in the generation dispatch of natural gas generation units is referred to the intra-day changes in the dispatch of these units in response to hour-to-hour changes in system demand that cannot be served by the renewable generation and other thermal generation technologies. Furthermore, despite knowing the direction of the natural gas flow, the Weymouth constraint is nonlinear [22]; therefore, linearization techniques were used to formulate the electricity network operation problem with natural gas system constraints as a mixed integer programming (MIP) problem with linear constraints [7],[8],[10].

In the electricity network, the unit commitment problem, which is solved by the independent system operator (ISO), involves binary decision variables that represent the commitment of the generation units. This problem has a discrete nonconvex feasibility region as a result of incorporated binary decision variables. The contributions of this paper are as follows: 1) develop an exact, tight, and computationally inexpensive convex relaxation for the short-term operation problem in electricity and natural gas networks; 2) propose a consensus optimization framework for the coordinated operation of the electricity and natural gas networks. The presented algorithm can be used by system operators to determine the tight convex relaxation of the operation problems that lead to global solutions for the short-term operation of electricity and natural gas networks. Furthermore, compared to earlier research [3],[4],[11],[20] that assumed the electricity network operator has access to the natural gas network information, the presented consensus optimization framework requires limited information being exchanged among the system operators. The rest of the paper is organized as follows, the problem formulation is presented in Section II. The convex relaxation of the proposed problems and the solution methodology is presented in Section III. A case study is presented in Section IV to show the effectiveness of the proposed relaxations. The conclusion is presented in Section V.

II. Problem Formulation

In this section, the short-term operation problems for the natural gas and electricity networks are formulated and the challenges for solving the coordinated operation of these systems using the consensus optimization framework are discussed.

A. Short-term Operation of Natural Gas Network

The mathematical formulation for the natural gas network operation is presented in (1)-(8). The objective is to minimize the natural gas consumption cost and the objective function is formulated as shown in (1). The natural gas pipeline capacity constraint is given in (2). The natural gas supply volume at each resource is further limited by (3). The operation limits on the natural gas pressure at each junction are given in (4). The Weymouth equation presents the dependence of natural gas flow in the pipeline to the pressure at the junctions on both sides of the pipeline as given in (5) and (6) [23]-[24]. The nodal natural gas flow balance at each junction is illustrated in (7) where $H_i(P_i)$ can be replaced by its piecewise linear form. The natural gas compressor is modeled as (8) [25].

$$\min \sum_t \sum_{s \in GS_j} \xi_s . v_{s,t} \quad (1)$$

$$-f_{j,o}^{p,\max} \le f_{j,o}^{p,t} \le f_{j,o}^{p,\max} \quad (2)$$

$$\underline{v}_s \le v_{s,t} \le \overline{v}_s \quad (3)$$

$$\underline{\pi} \le \pi_{j,t} \le \overline{\pi} \quad (4)$$

$$f_{j,o}^{p,t} = \mathrm{sgn}(\pi_{j,t}, \pi_{o,t}).C_{j,o}^{p} \sqrt{\left|\pi_{j,t} - \pi_{o,t}\right|} \quad (5)$$

$$\mathrm{sgn}(\pi_{j,t}, \pi_{o,t}) = \begin{cases} 1 & \pi_{j,t} \ge \pi_{o,t} \\ -1 & \pi_{j,t} < \pi_{o,t} \end{cases} \quad (6)$$

$$\sum_{s \in GS_j} A_j^s . v_{s,t} - \sum_{p \in P_{f,j}} f_{j,o}^{p,t} + \sum_{p \in P_{t,j}} f_{j,o}^{p,t} = \sum_{k \in HH_j} P_{k,t}^h + \sum_{i \in GG_j} H_i(P_{i,t}) \quad (7)$$

$$\pi_{j,t} \le \Gamma_{j,o}^{p} \pi_{o,t}, \qquad \Gamma_{j,o}^{p} \ge 1 \quad (8)$$

The presented problem is formulated as a mixed integer nonlinear optimization problem (MINLP). In order to determine the decision on the natural gas flow direction in the pipeline, (5)-(6) are further formulated as (9), where $u_{j,o}^{-,t}$ is a binary variable that is 1 if $\pi_{j,t} < \pi_{o,t}$ and is 0 if $\pi_{j,t} \ge \pi_{o,t}$. Therefore, the Weymouth equation represents a nonlinear non-convex constraint with discrete decision variables.

$$f_{j,o}^{p,t} = C_{j,o}^{p} \sqrt{\left|\pi_{j,t} - \pi_{o,t}\right|} - 2u_{j,o}^{-,t} C_{j,o}^{p} \sqrt{\left|\pi_{j,t} - \pi_{o,t}\right|} \quad (9)$$

B. *Short-term Operation of Electricity Network*

The short-term operation problem for the electricity network is formulated in (10)-(17) as a unit commitment problem. As shown in (10), the objective is to minimize the operation cost of the system. The objective function is the summation of the operation costs of all generation units. The generation dispatch of each generation unit is limited by the minimum and maximum capacity of the unit as shown in (11). Minimum up/downtime constraints are given in (12)-(13). The ramp up/down limits are enforced by (14)-(15). It is assumed that unit i sets at minimum generation $\underline{P}_i$ prior to shutting down and after starting up. The system-wide generation and demand balance is shown in (16). The power flow on the transmission line l is limited by (17), considering the respective shift factors that relate the power flow of the transmission line to the nodal injected power.

$$\min_{P_i, I_i} \sum_t \sum_i \left(\alpha_i P_{i,t}^2 + \beta_i P_{i,t} + \gamma_i I_{i,t} \right) \quad (10)$$

$$\underline{P}_i . I_{i,t} \le P_{i,t} \le \overline{P}_i . I_{i,t} \quad (11)$$

$$\left[X_{i,(t-1)}^{on} - T_i^{on} \right] \cdot \left[I_{i,(t-1)} - I_{i,t} \right] \ge 0 \quad (12)$$

$$\left[X_{i,(t-1)}^{off} - T_i^{off} \right] \cdot \left[I_{i,(t-1)} - I_{i,t} \right] \ge 0 \quad (13)$$

$$0 \le P_{i,t} - P_{i,(t-1)} \le \begin{pmatrix} (1 - (I_{i,t} - I_{i,(t-1)})).RU_i^{\max} \\ +(I_{i,t} - I_{i,(t-1)})\underline{P}_i \end{pmatrix} \quad (14)$$

$$0 \le P_{i,(t-1)} - P_{i,t} \le \begin{pmatrix} (1 - (I_{i,(t-1)} - I_{i,t})).RD_i^{\max} \\ +(I_{i,(t-1)} - I_{i,t})\underline{P}_i \end{pmatrix} \quad (15)$$

$$\sum_b P_{b,t}^D = \sum_i P_{i,t} \quad (16)$$

$$-\overline{F}_l \le \sum_b \left(\left(\sum_{i \in B_b} SF_l^b . P_{i,t} \right) - SF_l^b . P_{b,t}^D \right) \le \overline{F}_l \quad (17)$$

III. Proposed Convex Relaxation

A. *Background*

A theoretically strong convex relaxation that leverages the moment relaxation is proposed in [26]. The first order of moment relaxation represents the semi-definite relaxation of the original problem and as the order of the moment relaxation increases, the asymptotic convergence to the global optimal solution for the relaxed problem is guaranteed in polynomial time [26]. However, the increase in the number of variables in the moment relaxation matrices will lead to a considerable computational burden that impedes the utilization of such relaxations in practice.

By employing the chordal property of the electricity network graph, a sparse moment relaxation is formulated in [27]. Despite the fact that the sparse formulation is a step forward to practically utilize the theoretically perfect moment relaxation approach, the computational burden is still an obstacle even for the sparse formulation presented for the medium-sized networks [27]. The solution procured by formulating lower order moment relaxations is computationally less expensive compared to those for higher order moment relaxations; however, such solutions are not feasible for the original problem unless the rank of the moment matrix is one. If the rank of a moment matrix is larger than 1, a higher order of moment relaxation is required [26]. In such cases, the procured solution with a higher rank of the moment matrix is a lower (upper) bound – yet infeasible solution – for the expected global optimal solution of the minimization (maximization) problem. Since utilizing the higher order of moment relaxation is computationally expensive, the alternative is to employ perturbation to procure a rank-1 solution for the first order moment relaxation problem. However, the perturbation will lead to a rank-1 solution which renders a feasible yet not necessarily optimal solution for the original problem. Another approach to reducing the rank of the first order moment relaxation is to add valid constraints that include the elements of the first order moment relaxation matrix [28]. An example of such valid constraints is the McCormick and disjunctive constraints. Although valid constraints will help to reduce the rank of the first order moment relaxation matrix, the rank reduction may not lead to a rank-1 solution (i.e. the optimal solution that is feasible for the original non-convex problem.) Therefore, it is vital to develop a comprehensive approach to procuring a computationally inexpensive tight convex relaxation that renders a rank-1 solution by incorporating the lessons learned from the earlier attempts.

As shown in the natural gas and electricity network operation problems, the binary decision variables introduce non-convexity in the feasibility region. In order to handle these

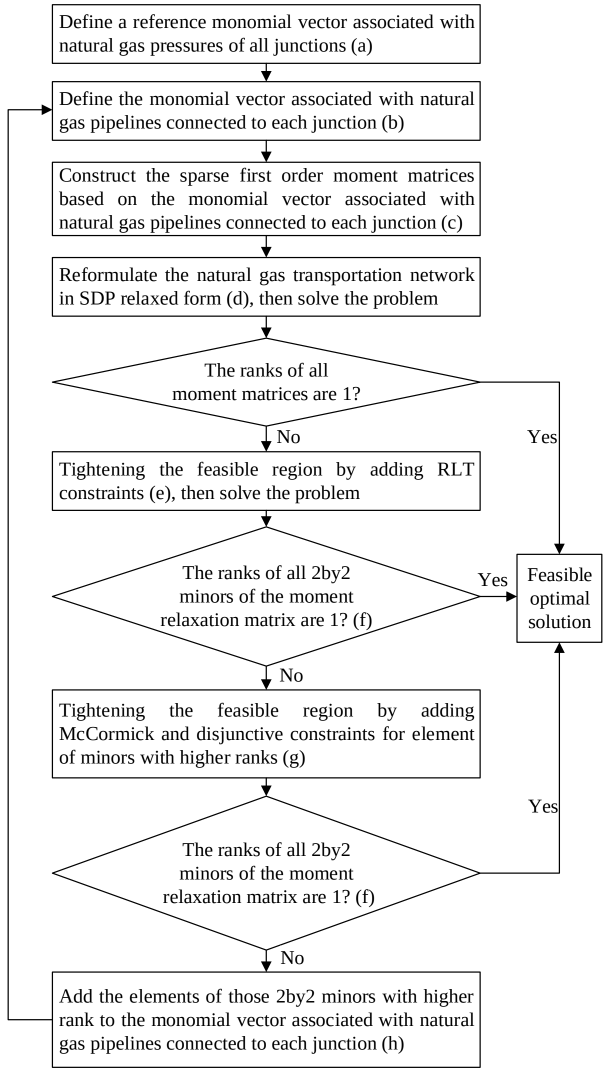

Fig. 1. The algorithm to procure an optimal solution for the natural gas network operation problem.

variables, the binary decision variables are characterized by introducing constraints (18)-(19). For the sake of simplicity, the index of hour t is eliminated from the presented formulation.

$$0 \le I^r \le 1 \tag{18}$$

$$I^r = \left(I^r\right)^2 \tag{19}$$

By using (18)-(19), the constraints (9) and (11) with discrete decision variables are transformed into nonlinear and nonconvex constraints with continuous decision variables (I^r). Incorporating (18)-(19) in (10)-(17) and (1)-(8) will lead to an NLP problem that is NP-hard with no guarantee for global or local optimal solution in polynomial time. In the next section, tight convex relaxations of the presented operation problems in electricity and natural gas networks will be formulated. The solution to the formulated relaxed problems is the solution to the original problem.

B. Convex Relaxation of Natural Gas Network Operation Problem

The non-convexity associated with the operation of the natural gas network is because of introducing constraint (9). Fig. 1 shows the developed algorithm to solve the short-term operation problem for the natural gas network. The steps of this algorithm are further described as follows:

Step (a) Define a reference vector of the first order monomials for the pressure of all junctions as given in (20).

$$\boldsymbol{\pi} = [\pi_1 \ \ \pi_2 \qquad .... \qquad \pi_{NJ}] \tag{20}$$

Step (b) Define monomials associated with the pipelines connected to each junction as given in (21). Such monomials could be further expanded in the solution procedure.

$$\mathbf{x}_j = [1 \ \ \mathbf{y}_{\bar{u}_{j,o}} \quad \mathbf{y}_{\sqrt{|\pi_j-\pi_o|}} \quad \mathbf{y}_{(\bar{u}_{j,o}\sqrt{|\pi_j-\pi_o|})}] \tag{21}$$

Here, $\mathbf{y}_{(.)}$ represents the lifting variable associated with the nonlinear terms in the non-convex optimization problem. For example, $\mathbf{y}_{\sqrt{|\pi_j-\pi_o|}}$ is the lifting variable that represents the nonlinear term $\sqrt{|\pi_j-\pi_o|}$. Therefore, the nonlinear terms are substituted in the relaxed formulation using the corresponding lifting variables $\mathbf{y}_{(.)}$. The general representation of the vector of monomials is given in (21). The first element in this vector is 1 which represents the normalization of the monomial. The second vector is the monomials associated with the direction of each pipeline that connects junctions j and o . It should be noted that if the direction is a priori, the binary decision variable $\bar{u}_{j,o}$ in monomials will be fixed. The third vector of monomials represents the nonlinear relationship among nodal gas pressure at both sides of the natural gas pipeline. This vector of monomials is formed for all pipelines that are connected to each junction regardless of the decision on the direction of natural gas flow in them. The fourth monomial vector is introduced to represent the binary to continuous terms associated with all the pipelines that are connected to the junction j , where The elements of the monomial vector only capture the pipelines for which the decision on the natural gas flow ($\bar{u}_{j,o}$) is a variable. Go to step (c).

Step (c) The moment matrix of the presented monomials for the junction j in (21), introduces a set of lifting variables as presented in (22).

$$\mathbf{X}_j = \begin{bmatrix} 1 & \mathbf{y}_{\bar{u}_{j,o}} & \mathbf{y}_{\sqrt{|\pi_j-\pi_o|}} & \mathbf{y}_{(\bar{u}_{j,o}\sqrt{|\pi_j-\pi_o|})} \\ \mathbf{y}_{\bar{u}_{j,o}} & \mathbf{y}_{\bar{u}_{j,o}} & \mathbf{y}_{(\bar{u}_{j,o}\sqrt{|\pi_j-\pi_o|})} & \mathbf{y}_{(\bar{u}_{j,o}\sqrt{|\pi_j-\pi_o|})} \\ \mathbf{y}_{\sqrt{|\pi_j-\pi_o|}} & \mathbf{y}_{(\bar{u}_{j,o}\sqrt{|\pi_j-\pi_o|})} & \pi_j-\pi_o+2\mathbf{y}_{(-\bar{u}_{j,o}(\pi_j-\pi_o))} & \mathbf{y}_{(-\bar{u}_{j,o}(\pi_j-\pi_o))} \\ \mathbf{y}_{(\bar{u}_{j,o}\sqrt{|\pi_j-\pi_o|})} & \mathbf{y}_{(\bar{u}_{j,o}\sqrt{|\pi_j-\pi_o|})} & \mathbf{y}_{(-\bar{u}_{j,o}(\pi_j-\pi_o))} & \mathbf{y}_{(-\bar{u}_{j,o}(\pi_j-\pi_o))} \end{bmatrix} \tag{22}$$

There are six types of independent variables in the moment matrix (22). Three of them (i.e. $\mathbf{y}_{\bar{u}_{j,o}}$, $\mathbf{y}_{\sqrt{|\pi_j-\pi_o|}}$, and $\mathbf{y}_{(\bar{u}_{j,o}\sqrt{|\pi_j-\pi_o|})}$) are the lifting variables given in (21). Two of them (i.e. π_j and π_o) are given in step (a) that are utilized in various moment matrices of each junction as represented by (20). The last variable (i.e. $\mathbf{y}_{(-\bar{u}_{j,o}(\pi_j-\pi_o))}$) is a lifting variable that is introduced in (22) to complete the moment matrix. Go to step (d).

Step (d) By utilizing the lifting variable that was introduced in step (c), the SDP relaxation for the short-term operation of the natural gas network given in (1)-(8) is reformulated as (23)-(28). Here the decision variables are the elements of the moment matrix (22) as well as the vector of pressure given in (20).

$$\min \quad \sum_{s\in GS_j} \xi_s . A_j^s \left(\sum_o C_{j,o}^p (\mathbf{y}_{\sqrt{|\pi_j-\pi_o|}}) \right) \tag{23}$$

$$-f_{j,o}^{p,\max} \le C_{j,o}^p (\mathbf{y}_{\sqrt{|\pi_j-\pi_o|}} - 2\mathbf{y}_{(u_{j,o}^- \sqrt{|\pi_j-\pi_o|})}) \le f_{j,o}^{p,\max} \tag{24}$$

$$\underline{v}_s \le A_j^s \left(\sum_o C_{j,o}^p (\mathbf{y}_{\sqrt{|\pi_j-\pi_o|}}) \right) \le \overline{v}_s \tag{25}$$

$$\underline{\pi} \le \pi_j \le \overline{\pi} \qquad \pi_j \le \Gamma_{j,o}^p \pi_o, \qquad \Gamma_{j,o}^p \ge 1 \tag{26}$$

$$\begin{aligned} &\sum_{s\in GS_j} A_j^s \left(\sum_o C_{j,o}^p (\mathbf{y}\sqrt{|\pi_j-\pi_o|}) \right) - \sum_{p\in P_{f,j}} C_{j,o}^p (\mathbf{y}\sqrt{|\pi_j-\pi_o|} - 2\mathbf{y}(u_{j,o}^- \sqrt{|\pi_j-\pi_o|})) + \\ &\sum_{p\in P_{t,j}} C_{j,o}^p (\mathbf{y}\sqrt{|\pi_j-\pi_o|} - 2\mathbf{y}(u_{j,o}^- \sqrt{|\pi_j-\pi_o|})) = \sum_{k\in HH_j} P_k^h + \sum_{i\in GG_j} H_i(P_i) \end{aligned} \tag{27}$$

$$\mathbf{X}_j \succeq 0 \tag{28}$$

The presented SDP problem is solved to determine the optimal solution for the original problem. If the rank of all sparse moment matrices associated with each junction is one, the procured optimal solution is feasible for the original non-convex problem (1)-(8). Otherwise, the algorithm proceeds to step (e) to further tighten the presented relaxation and to render rank-1 moment matrices.

Step (e) In this step, a tighter SDP relaxation is formulated by leveraging reformulation-linearization technique (RLT). The convex-relaxed problem (23)-(28) is presented in a compact form as shown in (29)-(34). The nodal balance constraint given in (27) is converted into two inequalities as shown in (30), (31). The inequalities given in (24)-(26) are also presented in the general form in (30)-(31). RLT is used to form valid constraints (32) and (33) to tighten the relaxation, while the moment matrices defined in step (c) (i.e. $\mathbf{X}_j$) and the monomials are given in step (b) (i.e. $\mathbf{x}_j$) are utilized to formulate these constraints.

$$\min_{\mathbf{x}_j, \mathbf{X}_j} \quad \sum_j \left(\xi_j^T \mathbf{x}_j \right) \tag{29}$$

$$\mathbf{g}_1^j \mathbf{x}_j - \mathbf{h}_1^j \ge 0 \tag{30}$$

$$\mathbf{g}_2^j \mathbf{x}_j - \mathbf{h}_2^j \le 0 \tag{31}$$

$$\mathbf{g}_1^j \mathbf{X}_j {\mathbf{g}_1^j}^T - \mathbf{h}_1^j {\mathbf{x}_j}^T {\mathbf{g}_1^j}^T - \mathbf{g}_1^j \mathbf{x}_j {\mathbf{h}_1^j}^T + \mathbf{h}_1^j {\mathbf{h}_1^j}^T \ge 0 \tag{32}$$

$$\mathbf{g}_2^j \mathbf{X}_j {\mathbf{g}_2^j}^T - \mathbf{h}_2^j {\mathbf{x}_j}^T {\mathbf{g}_2^j}^T - \mathbf{g}_2^j \mathbf{x}_j {\mathbf{h}_2^j}^T + \mathbf{h}_2^j {\mathbf{h}_2^j}^T \le 0 \tag{33}$$

$$\mathbf{X}_j \succeq 0 \tag{34}$$

Step (f) Solving the SDP relaxation problem with additional valid constraints will reduce the rank of the moment matrices corresponding to the procured solution (i.e. the lower bound to the optimal solution.) However, the rank of some of the sparse moment matrices may remain higher than one. To add a new set of valid constraints, it is necessary to exploit those elements of the moment matrix that result in the solution with a rank higher than 1. Theorem 1 is employed to identify such elements in moment matrices.

Theorem 1. *The rank of a moment relaxation matrix is one, if and only if the rank of all 2by2 minors (e.g.,* $\mathbf{X}_{j_{(i,k),(n,m)}}$ *where i, k, n, m are the indices for the rows and columns of* $\mathbf{X}_j$ *) of that matrix are one,* $rank(\mathbf{X}_j) = 1 \Leftrightarrow rank(\mathbf{X}_{j_{(i,k),(n,m)}}) = 1 \forall i,k,n,m$. The proof of this theorem is discussed in [28].

In this step, the ranks of all 2by2 minors are checked. If the ranks of all 2by2 minors are one, the convex relaxation is tight and the optimal solution for the original problem is procured. Otherwise, if the previous step was step (e) then go to step (g); if the previous step was step (g) then go to step (h).

Step (g) Once the minors with a rank higher than 1 are identified in step (f), McCormick constraints and disjunctive cuts are employed to reduce the rank of each minor within any moment matrix. The McCormick constraints for a bi-linear term xy are given in (35)-(38), where the upper and lower bounds of variable x and y are given as $\overline{x}, \overline{y}$ and $\underline{x}, \underline{y}$ respectively. This technique is applied to each term associated with the higher than rank-1 minors of each moment matrix.

$$xy \ge x \cdot \underline{y} + \underline{x} \cdot y - \underline{x} \cdot \underline{y} \tag{35}$$

$$xy \ge x \cdot \overline{y} + \overline{x} \cdot y - \overline{x} . \overline{y} \tag{36}$$

$$xy \le x \cdot \underline{y} + \overline{x} \cdot y - \overline{x} \cdot \underline{y} \tag{37}$$

$$xy \le x \cdot \overline{y} + \underline{x} \cdot y - \underline{x} \cdot \overline{y} \tag{38}$$

A list of such valid constraints are given in (40)-(43) and in the Appendix, where the scalar lifting variables that are used as the elements of the moment matrix (22) are captured. As an example here, the upper and lower bounds of $y_{(u_{j,o}^- \sqrt{|\pi_j-\pi_o|})}$ in the 2by2 minor given in (39) are presented in (40)-(43).

$$\begin{bmatrix} 1 & y_{(u_{j,o}^-)} \\ y_{(u_{j,o}^- \sqrt{|\pi_j-\pi_o|})} & y_{(u_{j,o}^- \sqrt{|\pi_j-\pi_o|})} \end{bmatrix} \tag{39}$$

Here, the lower and upper bounds of the off-diagonal elements in the 2by2 minor are $0 \le y_{(u_{j,o}^-)} \le 1$ and $0 \le y_{(\sqrt{|\pi_j-\pi_o|})} \le \sqrt{\overline{\pi}-\underline{\pi}}$. Using (35) and considering the lower bounds as zero for the off-diagonal elements, (40) is formed. All elements of the moment matrix are nonnegative. Similar to (36), the upper bounds of the off-diagonal elements of the 2by2 minor (39) are used in (41) to form a lower bound for the diagonal element ($y_{(u_{j,o}^- \sqrt{|\pi_j-\pi_o|})}$) in the 2by2 minor shown in (39). The upper bounds of the element $y_{(u_{j,o}^- \sqrt{|\pi_j-\pi_o|})}$ are enforced in (42)-(43) using the general form (37)-(38). As $0 \le y_{(u_{j,o}^-)} \le 1$, the upper bound of $y_{(u_{j,o}^- \sqrt{|\pi_j-\pi_o|})}$ is $y_{(\sqrt{|\pi_j-\pi_o|})}$ as given in (42). Using (37), $y_{(\sqrt{|\pi_j-\pi_o|})}$ and its upper bound ($\sqrt{\overline{\pi}-\underline{\pi}}$) are multiplied by zero which is the lower bound of $y_{(u_{j,o}^-)}$. Similarly, $y_{(\sqrt{|\pi_j-\pi_o|})}$ is multiplied by 1 which is the upper bound of $y_{(u_{j,o}^-)}$. Using (38), $y_{(u_{j,o}^-)}$ and its upper bound (i.e. 1) are multiplied by zero which is the lower

This is the author's version of an article that has been published in this journal. Changes were made to this version by the publisher prior to publication.
The final version of record is available at http://dx.doi.org/10.1109/TSG.2018.2825103

bound of $y_{(\sqrt{|\pi_j-\pi_o|})}$. Therefore, the only non-zero term in (43) is $y_{(u_{j,o}^-)}$ multiplied by $\sqrt{\bar{\pi}-\underline{\pi}}$ which is the upper bound of $y_{(\sqrt{|\pi_j-\pi_o|})}$. The rest of the valid constraints are presented in the Appendix.

$$y_{(u_{j,o}^-\sqrt{|\pi_j-\pi_o|})} \geq 0 \tag{40}$$

$$y_{(u_{j,o}^-\sqrt{|\pi_j-\pi_o|})} \geq y_{\sqrt{|\pi_j-\pi_o|}} - (\sqrt{\bar{\pi}-\underline{\pi}})(1-y_{u_{j,o}^-}) \tag{41}$$

$$y_{(u_{j,o}^-\sqrt{|\pi_j-\pi_o|})} \leq y_{\sqrt{|\pi_j-\pi_o|}} \tag{42}$$

$$y_{(u_{j,o}^-\sqrt{|\pi_j-\pi_o|})} \leq y_{u_{j,o}^-}(\sqrt{\bar{\pi}-\underline{\pi}}) \tag{43}$$

In this step, only the valid constraints associated with the 2by2 minors with a rank higher than 1 – that were determined in step (f) – will add more cutting planes to the feasible region of the problem to further tighten the relaxation. Go to step (f) to further check the rank of the 2by2 minors.

Step (h) The elements of the 2by2 minors with a rank higher than 1 will be added as new monomials to the vector of monomials in step (b). Traditionally, it is necessary to employ a higher order moment matrix to procure a rank-1 solution [26]. However, in this step, by applying Theorem 1, only certain elements that are present in the 2by2 minors with a rank higher than 1, will be added to the vector of monomials to tighten the feasible region of the procured moment relaxation. Therefore, instead of adding all elements of the higher order moment matrix for each junction, adding a limited number of monomial will not increase the size of the moment matrix dramatically. Go to step (b).

C. Convex Relaxation of the Electricity Network Operation Problem

The algorithm developed for the convex relaxation of this problem is similar to the algorithm developed for the natural gas network operation problem. The objective is to determine a tight convex relaxation for the electricity network operation problem considering the binary decision variables that represent the commitment of the generation units. The following steps are taken to achieve this objective.

Step (a) A vector of monomials is introduced as shown in (44).

$$\mathbf{z} = [1 \quad y_{I_1} \dots y_{I_{NG}} \quad y_{P_1} \quad \dots \quad y_{P_{NG}}] \tag{44}$$

Step (b) The associated first-order moment matrix of the presented monomials is given in (45) in which the binary-to-continuous terms are incorporated.

$$\mathbf{Z} = \begin{bmatrix} 1 & y_{I_1} & \cdots & y_{I_{NG}} & y_{P_1} & \cdots & y_{P_{NG}} \\ y_{I_1} & y_{I_1} & \cdots & y_{I_1 I_{NG}} & y_{I_1 P_1} & \cdots & y_{I_1 I_{NG}} \\ \cdots & \cdots & \cdots & \cdots & \cdots & \cdots & \cdots \\ y_{I_{NG}} & y_{I_1 I_{NG}} & \cdots & y_{I_{NG}} & y_{I_{NG} P_1} & \cdots & y_{I_{NG} P_{NG}} \\ y_{P_1} & y_{I_1 P_1} & \cdots & y_{I_{NG} P_1} & y_{P_1^2} & \cdots & y_{P_1 P_{NG}} \\ \cdots & \cdots & \cdots & \cdots & \cdots & \cdots & \cdots \\ y_{P_{NG}} & y_{I_1 P_{NG}} & \cdots & y_{I_{NG} P_{NG}} & y_{P_1 P_{NG}} & \cdots & y_{P_{NG}^2} \end{bmatrix} \tag{45}$$

Step (c) The lifting variables introduced in (45) are utilized to reformulate the electricity network operation problem (10)-(17) to (46)-(51). Here, the inequality constraints presented in (48)-(49) represent nodal power balance in the electricity network. If the rank of the moment matrix (45) is one, the procured lower bound solution is an optimal solution for the original problem and the algorithm will terminate, otherwise, proceed to step (d).

$$\min_{Z} \quad \sum_i \left(\alpha_i y_{P_i^2} + \beta_i y_{P_i} + \gamma_i y_{I_1}\right) \tag{46}$$

$$\underline{P}_i . y_{I_i} \leq y_{P_i} \leq \bar{P}_i . y_{I_i} \tag{47}$$

$$\sum_b P_b^D \leq \sum_i y_{I_i P_i} \tag{48}$$

$$\left(\sum_b P_b^D\right)^2 \geq \sum_{i'} \sum_i y_{P_i P_{i'}} \tag{49}$$

$$\underline{F}_l \leq \sum_b \left(\left(\sum_{i \in B_b} SF_l^b . y_{P_i} \right) - SF_l^b . P_b^D \right) \leq \bar{F}_l \tag{50}$$

$$\mathbf{Z} \succeq 0 \tag{51}$$

Step (d) Add the RLT constraints to tighten the procured relaxation. If the tightened relaxed problem renders a rank-1 solution, the procured lower bound is the optimal solution for the original problem. Otherwise, employ Theorem 1 to identify the minors with a rank higher than 1 and proceed to step (e).

Step (e) Once the 2by2 minors with a rank higher than 1, were identified, employ McCormick and disjunctive constraints to reduce their rank. This would also reduce the rank of the moment matrix introduced in step (b). By using these valid constraints, the size of the problem will not increase, however, the procured solution would be optimal for the original problem. If the relaxed problem that is tightened by adding the valid constraints procures a rank-1 solution, the algorithm is terminated. Otherwise, identify the 2by2 minors with higher than rank-1 and proceed to step (f).

Step (f) The elements of the minors with a rank higher than 1, are added to the vector of monomials introduced in step (a).

Using the proposed approach, the feasibility of the optimal solution to the convex-relaxed electricity network operation problem is guaranteed. With the increase in the order of the moment relaxation, the solution for the convex-relaxed problem will converge to the optimal solution of the original problem [23]. The proposed algorithm is computationally less expensive compared to employing higher order moment relaxation as it will only add the necessary elements to the vector of monomials to construct the moment matrix.

D. Coordination among Electricity and Natural Gas Networks Operation

Here, a consensus optimization framework is developed to capture the interactions among the natural gas and electricity networks. The presented consensus optimization is solved using the alternating direction method of multipliers (ADMM) [29]. The vector of shared variables among the natural gas and electricity networks is the volume of the natural gas demand for the natural gas generation units. The outline of the proposed problem is shown in (52)-(54). Here, $f(x)$ represents the objective function of the natural gas operation problem given in (23) and $g(z)$ represents the objective function of the electricity network operation problem given in (46). The convex-relaxed problems procured in sections III.B and III.C are represented by

(52) and (53) with feasible regions Ω_x and Ω_z respectively. Here, λ is the Lagrange multiplier of the consensus constraint.

$$Min \quad f(x) \quad s.t. \quad x \in \Omega_x, \quad x = z \quad : \lambda \tag{52}$$

$$Min \quad g(z) \quad s.t. \quad z \in \Omega_z, \quad z = x \quad : \lambda \tag{53}$$

The consensuses equality constraint is relaxed with respective Lagrange multiplier in the augmented Lagrangian function shown in (54) and ρ is a scalar.

$$L_\rho(x,z,\lambda) = f(x) + g(z) + \langle \lambda, x - z \rangle + \frac{\rho}{2}\|x - z\|_2^2 \tag{54}$$

In order to solve this problem, (52)-(53) are decomposed into two separate problems. The first problem (55) is the *x-update* problem and the second problem (56) is the *z-update* problem. As shown in (55), the *x-update* problem is solved in each iteration, while the variables associated with the *z-update* problem are fixed. Similarly, in the *z-update* problem (56) is solved while the variables associated with the *x-update* problem are fixed. Here, the *x-update* problem is the convex-relaxed natural gas network operation problem and the *z-update* is the convex-relaxed electricity network operation problem. The vector of Lagrange multipliers for the consensus constraints is updated in each iteration as shown in (57).

$$x^{\psi+1} \in \arg\min_{x \in \Omega_x} L_\rho(x, z^\psi, \lambda^\psi) \tag{55}$$

$$z^{\psi+1} \in \arg\min_{z \in \Omega_z} L_\rho(x^{\psi+1}, z, \lambda^\psi) \tag{56}$$

$$\lambda^{\psi+1} = \lambda^\psi + \rho(x^{\psi+1} - z^{\psi+1}) \tag{57}$$

IV. Case Study

A. 6-bus Power System

A sample 6-bus electricity network and 7-junction natural gas network are considered as shown in Fig. 2. The 6-bus electricity network is composed of 2 natural gas generation units (G1 and G2) and 1 fossil fuel generation unit (T1). The characteristics of the generation units and transmission lines are shown in Tables I and II, respectively. The fuel price of the thermal unit is \$3.5/MMBtu. The characteristics of the Natural gas resources and pipelines are shown in Tables III and IV, respectively. The minimum and maximum pressures at junctions of the natural gas network are 105 and 170 Psig respectively. The natural gas demands at junctions J1, J2, and J3 are 15%, 50% and 35% of the total natural gas demand, respectively. The electricity demand on buses 3, 4, and 5 are 20%, 40%, and 40% of the total electricity demand, respectively. The normalized demand profiles for the electricity and natural gas are given in Fig. 3. The peak demands for electricity and natural gas network are 256 MW at hour 17 and 6780 kcf at hour 20, respectively. Here, the numbers of binary variables in the natural gas and electricity network operation problems are 24 and 72 respectively. The numbers of continuous variables for the natural gas and electricity network operation problems are 504 and 216 respectively. The following four scenarios are presented:

Scenario 1) Uncoordinated operation of the electricity and natural gas networks

Scenario 2) Coordinated operation of the electricity and natural gas networks

Scenario 3) Scenario 2 with congestion in the electricity network

Scenario 4) Scenario 3 with congestion in the natural gas

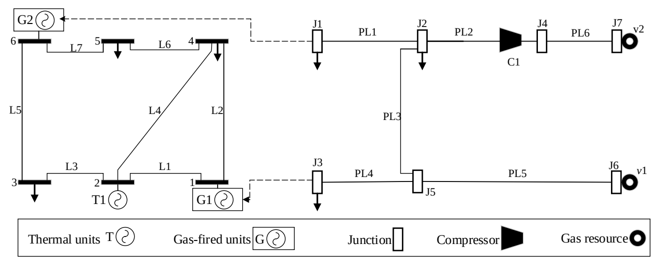

Fig. 2. The 6 bus-system interconnected with 7-junction natural gas

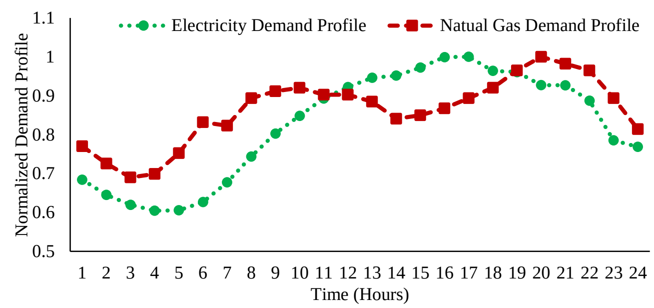

Fig. 3. The normalized demand profile for electricity and natural gas network

TABLE I
GENERATION UNIT CHARACTERISTICS

Unit	a (MMBtu/MWh²)	b (MMBtu/MWh)	c (MMBtu/h)	P_{min} (MW)	P_{max} (MW)	RU/RD (MW/h)	T_i^{on}, T_i^{off} (h)
G1	0.028	12.196	170.48	10	320	100,100	2,2
T1	0.0676	18.543	289.9	50	160	50,50	4,3
G2	0.058	10.69	136.29	10	60	50,50	1,1

TABLE II
TRANSMISSION LINE CHARACTERISTICS

Line ID	From Bus	To Bus	Impedance (p.u.)	Ling Rating (MW)
L1	1	2	0.170	80
L2	1	4	0.258	80
L3	2	4	0.197	70
L4	5	6	0.140	60
L5	3	6	0.018	80
L6	2	3	0.037	150
L7	4	5	0.037	70

TABLE III
NATURAL GAS RESOURCE CHARACTERISTICS

Resource	Minimum Capacity (kcf/h)	Maximum Capacity (kcf/h)	Cost (\$/kcf)
v1	1500	5000	2.6
v2	1000	6000	3.2

TABLE IV
NATURAL GAS PIPELINE CHARACTERISTICS

Line ID	From Junction	To Junction	Pipeline Constant (kcf /Psig)	Compressor factor
PL1	J1	J2	51	0
PL2	J2	J4	0	1.21
PL3	J2	J5	83	0
PL4	J3	J5	64	0
PL5	J5	J6	44	0
PL6	J4	J7	63	0

1) *Scenario 1 – Uncoordinated operation of the electricity and natural gas networks*

The hourly unit commitment solution is presented in Table V. At peak demand in hour 17, the generation dispatches of G1 and G2 are 196 MW and 60 MW, respectively. The total operation cost of the electricity network is $298,722. The volumes of natural gas withdrawn from resources *v*1 and *v*2 at hour 17 are 5000 kcf and 5827.7 kcf respectively. The total operation cost of the natural gas network is $675,887 and junction pressures of this network are shown in Table VI.

TABLE V
HOURLY UNIT COMMITMENT IN SCENARIO 1

Unit	Hours (0-24)																								
G1	1	1	1	1	1	1	1	1	1	1	1	1	1	1	1	1	1	1	1	1	1	1	1	1	1
T1	0	0	0	0	0	0	0	0	0	0	0	0	0	0	0	0	0	0	0	0	0	0	0	0	0
G2	1	1	0	0	0	0	0	0	1	1	1	1	1	1	1	1	1	1	1	1	1	1	1	1	1

TABLE VI
NATURAL GAS PRESSURES IN SCENARIO 1 AT HOUR 17

Junction ID	J1	J2	J3	J4	J5	J6	J7
Pressure (Psig)	131.44	137.80	105.00	137.80	137.55	178.42	165.96

The increase in the natural gas supply to serve the natural gas generation units leads to the violation of the operation limits of the natural gas network. For example, to serve the 3565.58 kcf natural gas demand of G1, the pressure at junction J6 is increased to 178.42 psig, which is higher than the maximum limit. Thus, the natural gas network is unable to supply the natural gas generation units.

2) *Scenario 2 – Coordinated operation of the electricity and natural gas networks*

In this scenario, the operational planning of the electricity network is coordinated with that for the natural gas network. However, the capacity limits of the transmission lines and pipelines are relaxed to avoid any congestion. In this scenario, in addition to units G1 and G2, T1 which is a more expensive unit is also committed as shown in Table VII. Compared to scenario 1, unit T1 is committed at hours 16-20, and G2 is committed at hour 7.

At hour 17, all units are committed to serve the peak electricity demand. The generation dispatches of G1, T1 and G2 are 153.5 MW, 50 MW, and 52.5 MW respectively. The generation dispatches of natural gas units G1 and G2 are decreased compared to those in scenario 1. Furthermore, the volumes of natural gas withdrawn from resource *v*1 and *v*2 are 4883.82 kcf and 4871.62 kcf respectively. The junction pressures in the natural gas network are given in Table VIII. In this scenario, the shared variables among the electricity and natural gas networks are the consumption volumes of the natural gas generation units. At hour 17, the natural gas consumption volumes for G1 and G2 are 2701.97 MMBtu and 1067.38 MMBtu, respectively. The flow of natural gas in pipeline PL3 is 113.83 kcf/h from junction J5 to J2 and the junction pressures are within their operation limits.

The total operation cost of the electricity network is increased to $303,956 which is 1.75% higher than that in scenario 1. Furthermore, the total operation cost of the natural gas network is decreased to $661,132.

TABLE VII
HOURLY UNIT COMMITMENT IN SCENARIO 1

Unit	Hours (0-24)																								
G1	1	1	1	1	1	1	1	1	1	1	1	1	1	1	1	1	1	1	1	1	1	1	1	1	1
T1	0	0	0	0	0	0	0	0	0	0	0	0	0	0	0	0	0	1	1	1	1	0	0	0	0
G2	1	1	0	0	0	0	0	1	1	1	1	1	1	1	1	1	1	1	1	1	1	1	1	1	1

TABLE VIII
NATURAL GAS PRESSURES IN SCENARIO 2 AT HOUR 17

Junction ID	J1	J2	J3	J4	J5	J6	J7
Pressure (Psig)	122.91	128.76	105.00	128.76	128.76	170.00	150.19

In order to show the performance of the presented algorithm the characteristics of the sparse moment matrices associated with each junction of the natural gas network were considered. The procured convex relaxation is exact if the rank of the all moment relaxation matrices is one. If the rank of a matrix is one, all of its eigenvalues are zero but one. Alternatively, if the ratio of the largest eigenvalue to the second largest eigenvalue of the moment matrix is very large (close to infinity), the rank of the matrix is one. Therefore, this ratio is used as a measure of the tightness for the proposed relaxation. The ratio of the two largest eigenvalues of the moment matrix associated with each junction of the natural gas network is evaluated for all hours in the operation horizon. As an example, this ratio is given for scenario 2 at peak hour (hour 17) in Table IX. Here, the rank-1 moment relaxation matrix corresponding to junction J4 is procure in step (d) of the algorithm before adding any RLT constraints, or new variables to the vector of monomials. However, the rank-1 moment relaxation matrices associated with junctions J6 and J7 are procured after adding the RLT constraints in step (e). Once the valid constraints added in step (g), the rank-1 moment relaxation matrix is procured for junctions J1 and J3. Finally, the rank-1 moment relaxation matrix is procured at step (h) for junctions J2 and J5 for which the variables associated with the rank higher than 1 2by2 minors are added to the vector of monomials in addition to the constraints added in the previous steps. YALMIP [30] is used to solve the problem and Mosek 7 is used as the SDP solver on a PC with 3.2 GHz Intel i5 processor and 8 GB of memory. The computation times for solving SDP problem at the last iteration of the ADMM approach to reach the optimal solution for 7-junction natural gas and 6-bus electricity network operation problems are 14.65 sec and 100.62 sec respectively. The total computation time to converge to a solution using the ADMM approach is 829.94 sec.

TABLE IX
THE RATIO OF THE TWO LARGEST EIGENVALUES IN SCENARIO 2 AT HOUR 17

Junction ID	J1	J2	J3	J4	J5	J6	J7
Step (d)	5.7E1	2.1E0	4.3E1	1.7E9	1.8E0	6.4E2	3.8E2
Step (e)	7.8E2	1.6E1	1.5E2	-	2.3E1	9.8E9	1.5E10
Step (g)	7.9E12	7.3E3	9.2E10	-	6.5E2	-	-
Step (h)	-	9.4E11	-	-	8.3E9	-	-

3) *Scenario 3 – Scenario 2 with Congestion in the Electricity Network*

In this scenario, the capacity limits of the pipelines are relaxed to avoid congestions in the natural gas network, and the power flow limits given in Table II are enforced for the electricity network. As shown in Table X, the generation units are committed for more number of hours compared to scenario 2 to avoid congestion in the electricity network. Compared to

This is the author's version of an article that has been published in this journal. Changes were made to this version by the publisher prior to publication.
The final version of record is available at http://dx.doi.org/10.1109/TSG.2018.2825103

scenario 2, the more expensive generation unit T1 is committed at hours 10-15 and 21-22 while the natural gas unit G2 is committed at hours 2-6. The total operation cost of electricity network is increased to $313,817, which is 3.24% higher than that in scenario 2.

TABLE X
HOURLY UNIT COMMITMENT OF SCENARIO 3

Unit	Hours (0-24)																								
G1	1	1	1	1	1	1	1	1	1	1	1	1	1	1	1	1	1	1	1	1	1	1	1	1	1
T1	0	0	0	0	0	0	0	0	0	0	0	1	1	1	1	1	1	1	1	1	1	1	1	0	0
G2	1	1	1	1	1	1	1	1	1	1	1	1	1	1	1	1	1	1	1	1	1	1	1	1	1

The decrease in the total dispatch of the natural gas generation units leads to the decrease in consumption in the natural gas network. The total operation cost of the natural gas network is decreased to $631,587 which is 4.46% less than that in scenario 2. At this hour, the volumes of natural gas withdrawn from the resources $v1$ and $v2$ are 5000 kcf and 4587.1 kcf, respectively. The total volume of natural gas withdrawn is decreased compared to scenario 2 as the overall natural gas consumption of the natural gas generation units is decreased. The junction pressures in the natural gas network at hour 17 are given in Table XI. The natural gas consumptions for G1 and G2 at hour 17 are 1792.3 MMBtu and 272.81 MMBtu, respectively. Compared to scenario 2, it is shown that congestion in the electricity network leads to the changes in the demand of the natural gas generation units. At hour 17, the flow of natural gas in pipeline PL3 is 554.15 kcf/h from junction J5 to J2 and the junction pressures are within the operation limits.

TABLE XI
PRESSURE AT JUNCTIONS IN SCENARIO 3 AT HOUR 17

Junction ID	J1	J2	J3	J4	J5	J6	J7
Pressure (Psig)	118.71	125.72	105.0	125.72	125.9	169.6	145.28

The ratio of the two largest eigenvalues of the moment relaxation matrix associated with each junction of the natural gas network at hour 17 in scenario 3 is considered as a tightness measure for the proposed convex relaxation as given in Table XII. Here, the rank-1 moment relaxation matrix corresponding to junction J4 is procured in step (d) of the algorithm. Adding RLT constraints in step (e) would lead to the rank-1 moment relaxation matrices corresponding to junctions J6 and J7. The rank-1 moment relaxation matrices corresponding to junctions J1, J2 and J3 are procured after adding the related valid constraints in step (g). Finally, the rank-1 moment relaxation is procured in step (h) for junction J5, where the variables associated with higher than 1 rank 2by2 minors are added to the vector of monomials in addition to the constraints added in previous steps. Compared this scenario with scenario 2, it is shown that the rank-1 moment relaxation matrix corresponding to junction J2 is procured in step (g) in scenario 3 while that was procured in step (h) in scenario 2.

TABLE XII
THE RATIO OF THE TWO LARGEST EIGENVALUES IN SCENARIO 3 AT HOUR 17

Junction ID	J1	J2	J3	J4	J5	J6	J7
Step (d)	9.2E2	2.1E1	6.5E1	9.8E9	2.1E1	4.1E3	2.5E3
Step (e)	1.3E3	2.2E2	5.1E3	-	9.7E1	6.9E8	2.6E9
Step (g)	1.1E14	9.4E9	8.3E11	-	4.7E4	-	-
Step (h)	-	-	-	-	7.4E8	-	-

4) Scenario 4 – Scenario 3 with Congestion in the Natural Gas Network

In this scenario, the capacity of pipeline PL3 is limited to 500 kcf/h while the capacity limits of the transmission lines are also considered. The congestion in the natural gas network will change the generation dispatch for some hours but the commitment status of the generation units remains the same as scenario 4. The congestion in the natural gas network affects the volume of natural gas withdrawn from the resources. As the natural gas demand of G1 alleviates the congestion in the natural gas network, the natural gas price for G1 is lower than that for G2 in this scenario. Therefore, the total operation cost of electricity network is decreased to $278,239 which is 11.33% less than that in scenario 3. While the generation dispatch and natural gas demand of natural gas generation units remain the same as those in scenario 3, the total operation cost of the natural gas network is increased to $634,025 which is 0.39% more than that in scenario 3. At hour 17, the volume of the natural gas withdrawn from resource $v1$ is decreased to 4945.85 kcf and the volume of the natural gas withdrawn from resource $v2$ is increased to 4641.24 kcf. Although the resource $v1$ is cheaper compared to $v2$, the limited capacity of pipeline PL3 (500 kcf/h) will reduce the withdrawn volume of natural gas from this resource. The pressures at the junctions at hour 17 are given in Table XIII. The efficiency of the presented algorithm for tightening the convex relaxation in this scenario is shown in Table XIV.

TABLE XIII
PRESSURE AT JUNCTIONS IN SCENARIO 4 AT HOUR 17

Junction ID	J1	J2	J3	J4	J5	J6	J7
Pressure (Psig)	118.75	125.75	105.0	125.75	125.90	168.78	145.74

TABLE XIV
THE RATIO OF THE TWO LARGEST EIGENVALUES IN SCENARIO 4 AT HOUR 17

Junction ID	J1	J2	J3	J4	J5	J6	J7
Step (d)	7.6E2	3.4E1	1.5E0	8.2E9	9.4E1	3.9E3	3.5E3
Step (e)	9.7E2	3.8E2	6.1E3	-	2.2E2	7.4E8	7.2E9
Step (g)	2.7E13	2.3E10	9.8E10	-	6.9E8	-	-
Step (h)	-	-	-	-	-	-	-

5) Discussion

The generation profiles of the generation units G1, G2, and T1 in scenarios are presented in Fig. 4, Fig. 5, and Fig. 6, respectively. By comparing scenarios 1 and 2, it is shown that the coordination among the electricity and natural gas networks will decrease the generation dispatch of the natural gas generation units at hours where the natural gas demand is increased in the network. During hours 16-20 the generation dispatch of G1 is decreased in scenario 2 compared to scenario 1 as shown in Fig. 4; and the generation dispatch of T1 is increased as shown in Fig. 6. A comparison of scenarios 2 and 3 highlights the impact of congestion within the electricity network on the dispatch profile of the generation units. As shown in Fig. 4, the generation dispatch of G1 is decreased during hours 2-6 while the generation dispatch of G2 is increased in the same period as shown in Fig. 5. Additionally, the generation dispatch of T1 is increased during hours 10-18. Comparing scenarios 3 and 4 shows the impact of congestion in the natural gas network on the generation dispatch of the generation units in the electricity network. As congestion in the natural gas network will decrease the marginal cost of the

This is the author's version of an article that has been published in this journal. Changes were made to this version by the publisher prior to publication.
The final version of record is available at http://dx.doi.org/10.1109/TSG.2018.2825103

generation unit G1 during hours 2-6, the generation dispatch of G1 will increase compared to that in scenario 3. The generation dispatch of G2 decreases accordingly. By comparing the

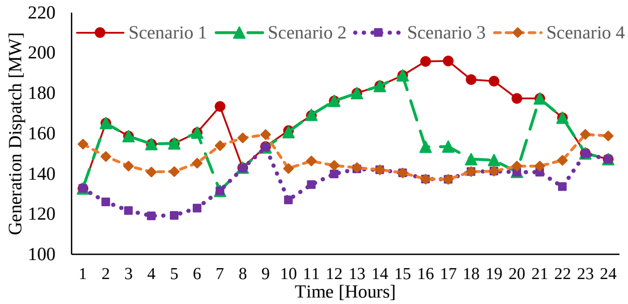

Fig. 4. The generation dispatch of G1 in scenarios

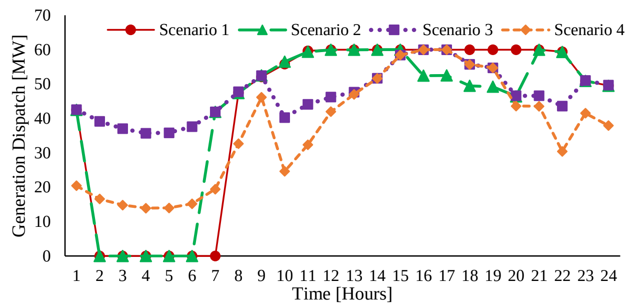

Fig. 5. The generation dispatch of G2 in scenarios

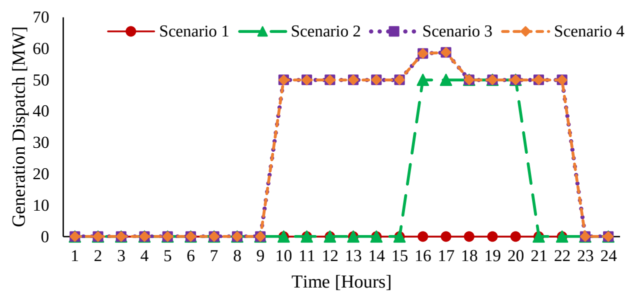

Fig. 6. The generation dispatch of T1 in scenarios

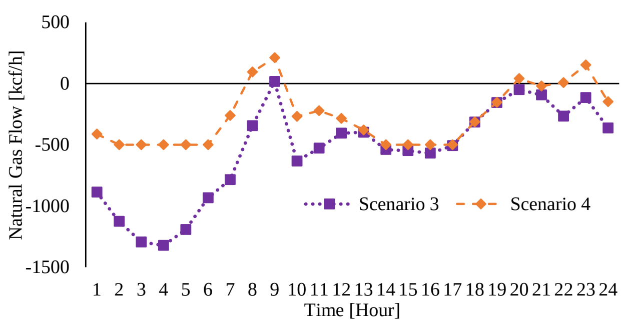

Fig. 7. The flow of natural gas in pipeline PL3 in scenarios 3-4.

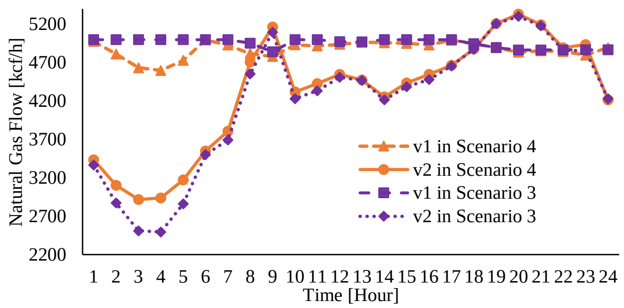

Fig. 8. The profile for the natural gas volume withdrawn from sources in scenarios 3-4.

generation dispatch of G1 for scenarios 2, 3, and 4, it is shown that although congestion in the natural gas network will increase the dispatch of G1, the limited capacity of the transmission lines in the electricity network will limit the increase in the generation dispatch to avoid congestion in the electricity network.

Furthermore, the presented formulation captures the variability in the electricity and natural gas network by addressing the bi-directional flow of natural gas in the pipelines. Here, the flows of natural gas in pipeline PL3 in scenario 3 and scenario 4 are given Fig. 7. As the flow of natural gas in this pipeline is limited to 500 kcf/h in scenario 4, the variation in the generation dispatch of the natural gas generation units in Fig. 4-6 will result in multiple changes in the direction of the natural gas flow in the pipeline PL3 in the operation horizon. The presented framework procures the flow direction in the pipelines as a result of the variation in the generation dispatch of the natural gas generation units.

Moreover, the congestion in the natural gas and electricity networks will impact the volume of natural gas withdrawn from the natural gas resources. The hourly volumes of natural gas withdrawn from the sources *v1* and *v2* in scenarios 3 and 4 are shown in Fig. 8. In congestion period for natural gas network in scenario 4, the natural gas withdrawn from source *v1* is decreased compared to that in scenario 3 and the natural gas withdrawn from source *v2* increased to compensate for the shortage in the natural gas supply. As a result of congestion in the natural gas network, the total operation cost of this network is increased from $631,587 in scenario 3 to $634,025 in scenario 4. As the increase in the natural gas demand of G1 mitigates the congestion in the natural gas network, the dispatch of this generation unit is increased as shown in Fig. 4.

B. IEEE 118-Bus System with 12-junction Natural Gas network

In this case, a modified IEEE-118 bus system is supplied by a 12-junction natural gas network. The electricity network has 46 fossil fuel generation units, 8 natural gas generation units, 186 branches, and 91 demand entities. The total capacity of the natural gas generation is 575 MW. The peak load is 3700 MW which occurs at hour 21. The natural gas network that supplies the electricity network is composed of 12 junctions, 12 pipelines, two compressors, and 12 natural gas demand entities including the natural gas generation units as shown in Fig. 9. The natural gas peak demand of 14,500 kcf that occurs at hour 19. Here, the numbers of binary variables for the natural gas and electricity network operation problem are 168 and 3888 respectively. The number of continuous variables for the natural gas network operation problem is 648 and the number of continuous variables for the electricity network operation problem is 3888. In the last iteration of the ADMM approach, the computation time for solving the formulated SDP representation of the 12-junction natural gas network operation problem is 20.94 sec. Here, the proposed algorithm for the natural gas operation problem is used to determine the sparse formulation for the IEEE 118-bus network operation problem. The computation time for the large-scale electricity network is reduced by leveraging the sparse formulation of the unit commitment problem and the solution time is 160.1 sec.

This is the author's version of an article that has been published in this journal. Changes were made to this version by the publisher prior to publication.
The final version of record is available at http://dx.doi.org/10.1109/TSG.2018.2825103

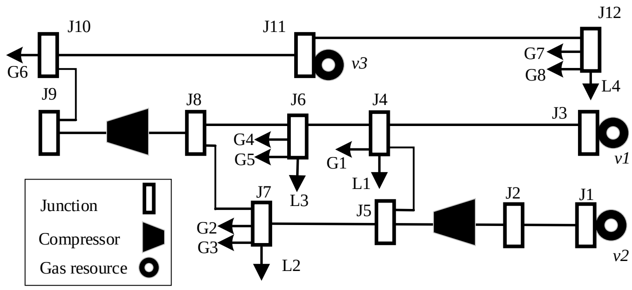

Fig. 9. 12-junction natural gas network

In this case study, the uncoordinated operation scheme (scenario 1) is compared to the coordinated operation scheme (scenario 2). As the natural gas network is constrained by the operation limits on the junction pressures, the natural gas generation units may not operate at their full capacity. As a result of imposing the pressure limits at junction J3, the dispatches of units G4 and G5 are decreased from 100 MW and 61.9 MW in scenario 1 to 76.3 MW and 0 MW at hour 21 in scenario 2, respectively. Here, as the natural gas demand increases the pressure at junctions will violate the operation limits. The natural gas pressure at junction J3 will increase to 172.9 psig at hour 21 which violates the upper limit for natural gas pressure at this junction. The commitment states of the generation units in scenario 1 are given in Table XV. Here the total operation cost is $1,603,326.

TABLE XV
HOURLY COMMITMENT IN SCENARIO 1

Unit	Hours (1-24)																							
T1-T3	0	0	0	0	0	0	0	0	0	0	0	0	0	0	0	0	0	0	0	0	0	0	0	0
T4-T5	1	1	1	1	1	1	1	1	1	1	1	1	1	1	1	1	1	1	1	1	1	1	1	1
T6	0	0	0	0	0	0	0	0	0	0	0	0	0	0	0	0	0	0	0	0	0	0	0	0
T7	0	0	0	0	0	0	1	1	1	1	1	1	1	1	1	1	1	1	1	1	1	1	1	1
T8-T9	0	0	0	0	0	0	0	0	0	0	0	0	0	0	0	0	0	0	0	0	0	0	0	0
T10-T11	1	1	1	1	1	1	1	1	1	1	1	1	1	1	1	1	1	1	1	1	1	1	1	1
T12	1	1	1	1	1	1	1	1	1	1	1	1	1	1	1	1	1	1	1	1	1	0	0	0
T13	0	0	0	0	0	0	0	0	0	0	0	0	0	0	0	0	0	0	0	0	0	0	0	0
T14	0	0	0	0	0	0	1	1	1	1	1	1	1	1	1	1	1	1	1	1	1	1	1	1
T15	0	0	0	0	0	0	0	0	0	0	0	0	0	0	0	0	0	0	0	0	0	0	0	0
T16	0	0	0	0	0	0	0	1	1	1	1	1	1	1	1	1	1	1	1	1	1	1	1	1
T17-T18	0	0	0	0	0	0	0	0	0	0	0	0	0	0	0	0	0	0	0	0	0	0	0	0
T19	0	0	0	0	0	0	0	0	1	1	1	1	1	1	1	1	1	1	1	1	1	1	1	1
T20-T21	1	1	1	1	1	1	1	1	1	1	1	1	1	1	1	1	1	1	1	1	1	1	1	1
T22-T23	0	0	0	0	0	0	0	0	1	1	1	1	1	1	1	1	1	1	1	1	1	1	1	1
T24-T25	1	1	1	1	1	1	1	1	1	1	1	1	1	1	1	1	1	1	1	1	1	1	1	1
T26	0	0	0	0	0	0	0	0	1	1	1	1	1	1	1	1	1	1	1	1	1	1	1	1
T27-T29	1	1	1	1	1	1	1	1	1	1	1	1	1	1	1	1	1	1	1	1	1	1	1	1
T30-T31	0	0	0	0	0	0	0	0	0	0	0	0	0	0	0	0	0	0	0	0	0	0	0	0
T32	0	0	0	0	0	0	0	1	1	1	1	1	1	1	1	1	1	1	1	1	1	1	1	1
T33	0	0	0	0	0	0	0	0	0	0	0	0	0	0	0	0	0	0	0	0	0	0	0	0
T34	0	0	0	0	0	0	0	0	0	0	0	0	0	0	1	1	1	1	1	1	1	1	1	1
T35-T36	1	1	1	1	1	1	1	1	1	1	1	1	1	1	1	1	1	1	1	1	1	1	1	1
T37	0	0	0	0	0	0	0	1	1	1	1	1	1	1	1	1	1	1	1	1	1	1	1	1
T38	0	0	0	0	0	0	0	0	0	0	0	0	0	0	0	0	0	0	0	0	0	0	0	0
T39-T40	1	1	1	1	1	1	1	1	1	1	1	1	1	1	1	1	1	1	1	1	1	1	1	1
T41-T42	0	0	0	0	0	0	0	0	0	0	0	0	0	0	0	0	0	0	0	0	0	0	0	0
T43-T45	1	1	1	1	1	1	1	1	1	1	1	1	1	1	1	1	1	1	1	1	1	1	1	1
T46	1	1	1	1	1	1	1	1	1	1	1	1	1	1	1	1	1	1	1	1	1	0	0	0
G1	1	1	1	1	1	1	1	1	1	1	1	1	1	1	1	1	1	1	1	1	1	1	1	1
G2	0	0	0	0	1	1	1	1	1	1	1	1	1	1	1	1	1	1	1	1	1	1	1	1
G3	0	0	0	0	0	0	1	1	1	1	1	1	1	1	1	1	1	1	1	1	1	1	1	1
G4	0	0	0	0	0	0	0	0	0	0	0	0	0	0	1	1	1	1	1	1	1	1	1	1
G5-G8	1	1	1	1	1	1	1	1	1	1	1	1	1	1	1	1	1	1	1	1	1	1	1	1

To ensure that the unit commitment solution in scenario 1 provides a feasible solution for the natural gas operation problem, the demands of the natural gas generation units are imposed to the natural gas network. In this case, the natural gas network failed to serve the demand of the natural gas generation units. In scenario 2, the operation of the electricity network is coordinated with the operation of the natural gas network. The changes in the commitment of the generation units compared to those in scenario 1 are given in Table XVI. Here, the total operation cost is increased to $1,629,829 which is 1.65% higher than that in scenario 1. However, unlike scenario 1, the presented solution for unit commitment is feasible for the natural gas network as there is no supply shortage for the natural gas generation units and there is no violation of the operation constraints of the natural gas network. Compared to scenario 1, the natural gas units G3 and G5 are not committed at hours 6-24 and 3-24 in scenario 2, respectively. Therefore, the more expensive fossil fuel units T13 and T34 are committed during hours 1-22 and 8-13, respectively. Moreover, G4 is committed at hours 5-13, G2 is committed at hour 4, T14 is decommitted in hour 8 and T46 is decommitted during hours 1-14 and 21-24.

TABLE XVI
CHANGES IN THE HOURLY COMMITMENT IN SCENARIO 2 FROM SCENARIO 1

Unit	Hours (1-24)																							
T13	1	1	1	1	1	1	1	1	1	1	1	1	1	1	1	1	1	1	1	1	1	0	0	0
T14	0	0	0	0	0	0	0	1	1	1	1	1	1	1	1	1	1	1	1	1	1	1	1	1
T34	0	0	0	0	0	0	0	0	1	1	1	1	1	1	1	1	1	1	1	1	1	1	1	1
T46	0	0	0	0	0	0	0	0	0	0	0	0	0	0	1	1	1	1	1	1	1	0	0	0
G2	0	0	0	1	1	1	1	1	1	1	1	1	1	1	1	1	1	1	1	1	1	1	1	1
G3	0	0	0	0	0	0	0	0	0	0	0	0	0	0	0	0	0	0	0	0	0	0	0	0
G4	0	0	0	0	1	1	1	1	1	1	1	1	1	1	1	1	1	1	1	1	1	1	1	1
G5	1	1	0	0	0	0	0	0	0	0	0	0	0	0	0	0	0	0	0	0	0	0	0	0

V. CONCLUSION

This paper presents a consensus optimization framework for the coordinated operation of electricity and natural gas networks. Tight convex relaxations for the electricity and natural gas operation problems with nonconvex feasible regions were proposed. The nonconvex feasible region is characterized by the Weymouth equation in the natural gas network, and the introduced unit commitment binary decision variables in the electricity network. A computationally tractable convex representation with several valid constraints is formulated that procures a rank-1 optimal solution for the natural gas and electricity network operation problems. The alternating direction method of multipliers is used to solve the convex-relaxed consensus optimization problem. Two case studies showed the effectiveness of the proposed approach to capture the interdependence among electricity and natural gas networks.

The presented approach exploits the sparsity of the natural gas network. If the natural gas network is dense, procuring the rank-1 moment relaxation matrix will be more challenging. Additionally, in order to reach the global solution, the number of monomials within the vector of monomials could increase dramatically. Consequently, a very large moment relaxation for each junction of the natural gas network is formed. Although the presented algorithm would avoid forming the unnecessary large moment relaxation matrices, very large moment relaxation matrices may be required to procure a rank-1 moment relaxation matrix. This work could be further extended to capture a more detailed model of the natural gas network considering the nonlinearities in power consumption of the compressors.

This is the author's version of an article that has been published in this journal. Changes were made to this version by the publisher prior to publication.
The final version of record is available at http://dx.doi.org/10.1109/TSG.2018.2825103

APPENDIX

A strategy similar to the utilized strategy for equations (40)-(43) is employed to formulate (A.1)-(A.20) according to the general form given in (35)-(38). In this formulation, it is assumed that junction j is connected to the junctions o and k. For instance, the valid constraints (A.7)-(A.9) incorporate the lifting variable $y_{u^{-}_{j,k}}$, that determines the direction of natural gas flow in the pipeline connecting junctions j and k.

$$y_{(-u^{-}_{j,o}(\pi_j-\pi_o))} \geq 2(\sqrt{\bar{\pi}-\underline{\pi}})y_{(u^{-}_{j,o}\sqrt{|\pi_j-\pi_o|})} - (\bar{\pi}-\underline{\pi}) \tag{A.1}$$

$$y_{(-u^{-}_{j,o}(\pi_j-\pi_o))} \leq \pi_j - \pi_o + (\bar{\pi}-\underline{\pi})(1-y_{u^{-}_{j,o}}) \tag{A.2}$$

$$y_{(-u^{-}_{j,o}(\pi_j-\pi_o))} \leq y_{(u^{-}_{j,o}\sqrt{|\pi_j-\pi_o|})}(\sqrt{\bar{\pi}-\underline{\pi}}) \tag{A.3}$$

$$\pi_j - \pi_o + 2y_{(-u^{-}_{j,o}(\pi_j-\pi_o))} \geq 2(\sqrt{\bar{\pi}-\underline{\pi}})y_{\sqrt{|\pi_j-\pi_o|}} - (\bar{\pi}-\underline{\pi}) \tag{A.4}$$

$$\pi_j - \pi_o + 2y_{(-u^{-}_{j,o}(\pi_j-\pi_o))} \leq (\sqrt{\bar{\pi}-\underline{\pi}})y_{\sqrt{|\pi_j-\pi_o|}} - (\bar{\pi}-\underline{\pi}) \tag{A.5}$$

$$\pi_j - \pi_o \leq y_{u^{-}_{j,o}}(\bar{\pi}-\underline{\pi}) \tag{A.6}$$

$$y_{(u^{-}_{j,k}\sqrt{|\pi_j-\pi_o|})} \geq y_{\sqrt{|\pi_j-\pi_o|}} - (\sqrt{\bar{\pi}-\underline{\pi}})(1-y_{u^{-}_{j,k}}) \tag{A.7}$$

$$y_{(u^{-}_{j,k}\sqrt{|\pi_j-\pi_o|})} \leq y_{\sqrt{|\pi_j-\pi_o|}} \tag{A.8}$$

$$y_{(u^{-}_{j,k}\sqrt{|\pi_j-\pi_o|})} \leq y_{u^{-}_{j,k}}(\sqrt{\bar{\pi}-\underline{\pi}}) \tag{A.9}$$

$$y_{(u^{-}_{j,o}\sqrt{|\pi_j-\pi_o|}\sqrt{|\pi_j-\pi_k|})} \geq y_{(u^{-}_{j,o}\sqrt{|\pi_j-\pi_o|})}(\sqrt{\bar{\pi}-\underline{\pi}}) + y_{\sqrt{|\pi_j-\pi_k|}}(\sqrt{\bar{\pi}-\underline{\pi}}) - (\bar{\pi}-\underline{\pi}) \tag{A.10}$$

$$y_{(u^{-}_{j,o}\sqrt{|\pi_j-\pi_o|}\sqrt{|\pi_j-\pi_k|})} \leq y_{(u^{-}_{j,o}\sqrt{|\pi_j-\pi_o|})}(\sqrt{\bar{\pi}-\underline{\pi}}) \tag{A.11}$$

$$y_{(u^{-}_{j,o}\sqrt{|\pi_j-\pi_o|}\sqrt{|\pi_j-\pi_k|})} \leq y_{\sqrt{|\pi_j-\pi_k|}}(\sqrt{\bar{\pi}-\underline{\pi}}) \tag{A.12}$$

$$\pi_j - \pi_o \leq y_{(\sqrt{|\pi_j-\pi_o|})}(\sqrt{\bar{\pi}-\underline{\pi}}) \tag{A.13}$$

$$\pi_j - \pi_o \geq 2y_{(\sqrt{|\pi_j-\pi_o|})}(\sqrt{\bar{\pi}-\underline{\pi}}) - (\bar{\pi}-\underline{\pi}) \tag{A.14}$$

$$y_{(\sqrt{|\pi_j-\pi_o|}\sqrt{|\pi_j-\pi_k|})} \geq y_{(\sqrt{|\pi_j-\pi_o|})}(\sqrt{\bar{\pi}-\underline{\pi}}) + y_{\sqrt{|\pi_j-\pi_k|}}(\sqrt{\bar{\pi}-\underline{\pi}}) - (\bar{\pi}-\underline{\pi}) \tag{A.15}$$

$$y_{(\sqrt{|\pi_j-\pi_o|}\sqrt{|\pi_j-\pi_k|})} \leq y_{(\sqrt{|\pi_j-\pi_o|})}(\sqrt{\bar{\pi}-\underline{\pi}}) \tag{A.16}$$

$$y_{(\sqrt{|\pi_j-\pi_o|}\sqrt{|\pi_j-\pi_k|})} \leq y_{\sqrt{|\pi_j-\pi_k|}}(\sqrt{\bar{\pi}-\underline{\pi}}) \tag{A.17}$$

$$y_{(u^{-}_{j,o}u^{-}_{j,k})} \geq y_{(u^{-}_{j,o})} + y_{(u^{-}_{j,k})} - 1 \tag{A.18}$$

$$y_{(u^{-}_{j,o}u^{-}_{j,k})} \leq y_{(u^{-}_{j,o})} \tag{A.19}$$

$$y_{(u^{-}_{j,o}u^{-}_{j,k})} \leq y_{(u^{-}_{j,k})} \tag{A.20}$$

REFERENCES

[1] M. Shahidehpour and Z. Li. White paper: Long-term electric and natural gas infrastructure requirements. Technical report, Illinois Institute of Technology, 2014.

[2] Forward Market Operations. Energy & Ancillary Services Market Operations, M-11 Rev. 75. Technical report, PJM, 2015.

[3] M. Shahidehpour, Y. Fu, and T. Wiedman, "Impact of natural gas infrastructure on electric power systems," *Proc. IEEE*, vol. 93, pp. 1042–1056, May 2005.

[4] M. Geidl and G. Andersson, "Optimal power flow of multiple energy carriers," *IEEE Trans. Power Syst.*, vol. 22, no. 1, pp. 145-155, 2007.

[5] G. Maria, P. Duenas, and J. Reneses, "Electricity and natural gas interdependency: comparison of two methodologies for coupling large market models within the European regulatory framework," *IEEE Trans. Power Syst.* vol. 31, no. 1, pp. 361-369, 2016.

[6] S. Bahram and A. Sheikhi, "From demand response in smart grid toward integrated demand response in smart energy hub, *IEEE Trans. Smart Grid*, vol. 7, no. 2, pp. 650-658, 2016.

[7] T. Li, M. Eremia, and M. Shahidehpour, "Interdependency of natural gas network and power system security," *IEEE Trans. Power Syst.*, vol. 23, no. 4, pp. 1817-1824, Nov. 2008.

[8] C. Shao, X. Wang, M. Shahidehpour, X. Wang, and B. Wang, "An MILP-Based Optimal Power Flow in Multicarrier Energy Systems," *IEEE Trans. Sust. Energy*, vol. 8, no.1, pp. 239-248, Jan. 2017.

[9] F. Wu, H. Nagarajan, A. Zlotnik, and R. Sioshansi, "adaptive convex relaxations for gas pipeline network optimization," *in proc. American Control Conference (ACC). IEEE*, 2017.

[10] A. Abdulwahab, A. Abusorrah, X. Zhang, and M. Shahidehpour, "Coordination of interdependent natural gas and electricity infrastructures for firming the variability of wind energy in stochastic day-ahead scheduling," *IEEE Trans. Sust. Energy*, vol. 6, no. 2, pp. 606-615, Apr. 2015.

[11] A. Martinez-Mares and F. R. Claudio, "A unified gas and power flow analysis in natural gas and electricity coupled networks." *IEEE Trans. Power Syst.* vol 27, no. 4, pp. 2156-2166, 2012.

[12] C. Liu, M. Shahidehpour, Y. Fu and Z. Li, "Security-Constrained Unit Commitment With Natural Gas Transmission Constraints," *IEEE Trans. Power Systems,*, vol. 24, pp. 1523-1536, 2009.

[13] M. Moeini-Aghtaie, A. Abbaspour, M. Fotuhi-Firuzabad, and E. Hajipour. "A decomposed solution to multiple-energy carriers optimal power flow." *IEEE Trans on Power Syst*, vol. 29, no. 2, pp. 707-716, 2014.

[14] C. Unsihuay-Vila, J. W. Marangon-Lima, A. C. Zambroni de Souza, I. J. Perez-Arriaga, and P. P. Balestrassi,, "A model to long-term, multiarea, multistage, and integrated expansion planning of electricity and natural gas systems," *IEEE Trans. Power Syst.*, vol. 25, no. 2, pp. 1154–1168, May 2010.

[15] A. Martinez-Mares and F. R. Claudio, "A robust optimization approach for the interdependency analysis of integrated energy systems considering wind power uncertainty," *IEEE Trans. Power Syst.*, vol. 28, no. 4, pp. 3964-3976, 2013.

[16] A. Zlotnik, L. Roald, S. Backhaus, M. Chertkov, and G. Andersson, "Coordinated scheduling for interdependent electric power and natural gas infrastructures," *IEEE Trans. on Power Systems*, vol. 32, no. 1, pp. 600–610, 2017.

[17] M. Qadrdan, J. Wu, N. Jenkins, and J. Ekanayake, "Operating strategies for a GB integrated gas and electricity network considering the uncertainty in wind power forecasts," *IEEE Trans. Sustain. Energy*, vol. 5, no. 1, pp. 128-138. Jan. 2014.

[18] C. He, L. Wu, T. Liu, and M. Shahidehpour, "Robust co-optimization scheduling of electricity and natural gas systems via admm," *IEEE Trans. Sustain. Ener.*, vol. pp, no. 99, pp. 1–12.

[19] Y. Wen, X. Qu, W. Li, X. Liu, X. Ye, "Synergistic Operation of Electricity and Natural Gas Networks via ADMM*," IEEE Trans. Smart Grid*, vol. PP, no.99, pp.1-1, 2017.

[20] C. M. Correa-Posada and P. Sanchez-Martin, "Security-constrained optimal power and natural-gas flow," *IEEE Trans. Power Syst.*, vol. 29, no. 4, pp. 1780-1787, Jul. 2014.

[21] P. J. Hibbard and T. Schatzki, "The interdependence of electricity and natural gas: Current factors and future prospects," *Electricity J.*, vol. 25, no. 4, pp. 6–17, May 2012.

[22] C. B. Sanchez, R. Bent, S. Backhaus, S. Blumsack, H. Hijazi, and P. van Hentenryck, "Convex optimization for joint expansion planning of natural gas and power systems*," in 49th Hawai'i Int'l. Conf. Sys. Sci.*, pp. 1–10, Jan 2016.

[23] E. S. Menon, Gas Pipeline Hydraulics. New York: Taylor & Francis, 2005.

[24] Compressible gas flow, Pipe Flow Calculations. [Online]. Available: http://www.pipeflowcalculations.com/pipe-valve-fitting-flow/compressible-gas-flow.php

[25] A. Tomasgard, F. Rømo, M. Fodstad, and K. Midthun, "Optimization models for the natural gas value chain," *Geom. Model., Numer. Simul., Optimiz.*, pp. 521-558, 2007.

[26] J.-B. Lasserre, Moments, Positive Polynomials and Their Applications. *Imperial College Press*, 2010.

[27] D. K. Molzahn and I. A. Hiskens, "Sparsity-exploiting moment-based relaxations of the optimal power flow problem," *IEEE Trans. Power Syst.*, vol. 30, no. 6, pp. 3168-3180, Nov. 2015.

[28] B. Kocuk, S. Dey, and A. Sun, "Strong SOCP relaxation for the optimal power flow problem," *Oper. Res.* Vol. 64, no. 6, pp. 1177-1196, Dec. 2016.
[29] S. Boyd, N. Parikh, E. Chu, B. Peleato, and J. Eckstein, "Distributed optimization and statistical learning via the alternating direction method of multipliers," *Foundations and Trends R in Machine Learning*, vol. 3, no. 1, pp. 1–122, 2011.
[30] J. Lofberg, "Yalmip: A toolbox for modeling and optimization in MATLAB," *in Proc. IEEE Int. Symp. Comput. Aided Control Syst. Des.*, Taipei, Taiwan, Sep. 2004, pp. 284–289.

Saeed D. Manshadi (S'14) received the B.S. degrees in electrical engineering from School of Electrical and Computer Engineering, University of Tehran, Tehran, Iran, in 2012 and the M.S. degree in electrical engineering from the University at Buffalo, the State University of New York (SUNY), Buffalo, NY, USA, in 2014. He is currently working toward the Ph.D. degree in electrical engineering at Southern Methodist University, Dallas, TX, USA. His research interests include microgrids, smart grid, and power system operation and planning.

Mohammad E. Khodayar (SM'17) received the B.Sc. degree from Amirkabir University of Technology, Tehran, Iran; the M.S. degree from Sharif University of Technology, Tehran; and the Ph.D. degree from the Illinois Institute of Technology, Chicago, IL, USA, in 2012, all in electrical engineering. He was a Senior Research Associate with the Robert W. Galvin Center for Electricity Innovation, Illinois Institute of Technology. He is currently an Assistant Professor in the Department of Electrical Engineering, Southern Methodist University, Dallas, TX, USA and an associate editor of the IEEE Transactions on Sustainable Energy and IEEE Transactions on Vehicular Technology. His current research interests include power system operation and planning.